

Triplet supercurrent due to spin-active zones in a Josephson junction

Jacob Linder¹ and Asle Sudbø¹

¹*Department of Physics, Norwegian University of Science and Technology, N-7491 Trondheim, Norway*

(Dated: January 24, 2017)

Motivated by a recent experiment evidencing triplet superconductivity in a ferromagnetic Josephson junction with a Cu_2MnAl -Heusler barrier, we construct a theoretical model accounting for this observation. The key ingredients in our model which generate the triplet supercurrent are *spin-active zones*, characterised by an effective canted interface magnetic moment. Using a numerical solution of the quasiclassical equations of superconductivity with spin-active boundary conditions, we find qualitatively very good agreement with the experimentally observed supercurrent. Further experimental implications of the spin-active zones are discussed.

PACS numbers: 74.20.Rp

Since the pioneering studies 50 years ago¹, the interplay between ferromagnetic (F) and superconducting (S) order has been much investigated, particularly so in recent years^{2,3}. This can largely be ascribed to important experimental developments which have allowed for microscopic studies of both artificially engineered⁴ and intrinsic coexistence⁵ of F and S order, in addition to theoretical advances. One of the most exciting prospects in hybrid F|S structures is the possibility of tailoring the desired properties of the system on a nanometer scale. To accomplish this, it is necessary to take seriously the influence of the interface properties. Depending on whether the interfaces have spin-dependent properties or not, exotic new features may come into play in F|S structures, including long-range Josephson effects⁶⁻⁸ and unconventional types of superconducting pairing⁹⁻¹¹.

In a very recent experiment by Sprungmann *et al.*¹², the importance of such interface properties was underscored. A long-range triplet supercurrent was observed in a S|F|S Josephson junction with a Cu_2MnAl -Heusler barrier acting as the F region. Surprisingly, Sprungmann *et al.* observed a conventional, exponentially decaying supercurrent in the as-prepared state of the Cu_2MnAl layer, whereas a long-range supercurrent virtually independent of the junction thickness (up to a critical value) was observed upon annealing the junction. Beyond a critical value of the junction-thickness, an unusual abrupt decay of the supercurrent was observed. In the annealed case, the Heusler layer acquires a ferromagnetic order in its core, but retains spin glass order near the interfaces in the thickness range just above the onset of ferromagnetism. Therefore, it was suggested in Ref.¹² that the coupling between ferromagnetic and spin glass order would lead to a canted magnetization texture near the interfaces, which could be the necessary mechanism responsible for the observed triplet supercurrent. Illuminating this matter would be important to understand further the role of spin-active zones in Josephson junctions and their possible manipulation, which in turn could lead to tunable long-range supercurrents.

In this Rapid Communication, we construct a theoretical model to explain the experimental finding in Ref.¹² by including the role of canted magnetic interface moments in the quasiclassical theory of superconductivity. Employing a numerical solution in the diffusive regime of transport, we obtain very good qualitative agreement with observed supercurrent

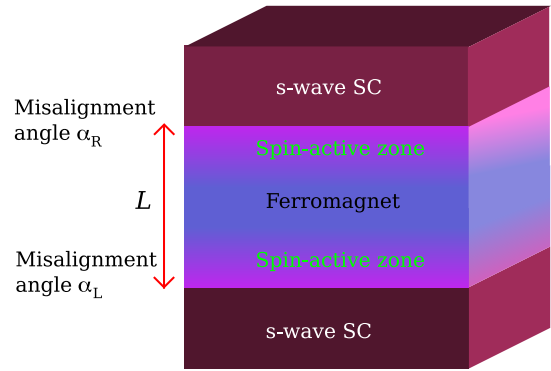


FIG. 1: (Color online) The model employed for a Josephson junction with a ferromagnetic Heusler Cu_2MnAl barrier. The junction width is L , and we take into account a canted magnetization texture near the interfaces with misalignment angles $\alpha_{L,R}$ relative the bulk magnetization. These spin-active zones generate a long-range supercurrent.

in Ref.¹². Moreover, we highlight additional implications of spin-active zones in a Josephson junction. In particular, we find that if these zones couple together in a parallel alignment, *the total supercurrent may actually vanish* for certain misalignment angles of the canted magnetic moments. Our results demonstrate the significance of spin-active zones in ferromagnetic Josephson junctions, and may provide a guideline for interpretation of experimental data and future investigations of such heterostructures.

The system under consideration is shown in Fig. 1. A ferromagnetic region of width L is sandwiched between two standard *s*-wave superconductors (*e.g.* Nb). Near the interfaces, we identify *spin-active zones* which may arise *e.g.* due to the presence of magnetic disorder or canted magnetic moments which are misaligned compared to the bulk magnetization direction. To study this system, we employ the quasiclassical theory of superconductivity which provides equations of motion for the Green's functions of the system. By supplementing these equations with proper boundary conditions for spin-active interfaces with possibly misaligned magnetic moments, we are able to compute the supercurrent flowing through the system. We give a brief account of the theoretical framework here, and refer the reader to *e.g.* Ref.² for a comprehensive review. In the F region, we employ a Ricatti-parametrization¹⁴

of the Green's function as follows

$$\hat{g} = \begin{pmatrix} \underline{\mathcal{N}}(1 - \underline{\tilde{\gamma}}) & 2\underline{\mathcal{N}}\underline{\gamma} \\ 2\underline{\tilde{\mathcal{N}}}\underline{\tilde{\gamma}} & \underline{\tilde{\mathcal{N}}}(-1 + \underline{\tilde{\gamma}}) \end{pmatrix}, \quad (1)$$

where $\underline{\mathcal{N}} = (1 + \underline{\tilde{\gamma}})^{-1}$ and $\underline{\tilde{\mathcal{N}}} = (1 + \underline{\tilde{\gamma}})^{-1}$. It also satisfies $(\hat{g})^2 = \hat{1}$, and is characterized by the two unknown 2×2 matrices $\underline{\gamma}$ and $\underline{\tilde{\gamma}}$. The above Green's functions satisfy the Usadel equation¹⁵

$$\mathcal{D}\hat{g}\partial_x\hat{g} + i[\varepsilon\hat{p}_3 + h\text{diag}(\underline{\tau}_3, \underline{\tau}_3), \hat{g}] = 0. \quad (2)$$

Here, \mathcal{D} is the diffusion coefficient in the F region, h is the magnitude of the exchange field, while ε is the quasiparticle energy. To obtain a complete solution of the Green's function, it is necessary to supplement the Usadel equation with boundary conditions¹⁶. Assuming that the F region extends from $x = 0$ to $x = L$, the boundary conditions read

$$\begin{aligned} 2\underline{\gamma}_T^l L \hat{g} \partial_x \hat{g} &= [\hat{g}^l, \hat{g}] + i\underline{\gamma}_s^l [\hat{M}(\alpha_L), \hat{g}] \text{ at } x = 0, \\ 2\underline{\gamma}_T^r L \hat{g} \partial_x \hat{g} &= [\hat{g}, \hat{g}^r] - i\underline{\gamma}_s^r [\hat{M}(\alpha_R), \hat{g}] \text{ at } x = L. \end{aligned} \quad (3)$$

Here, we have introduced

$$\hat{M}(\alpha) = (\cos \alpha) \text{diag}(\underline{\sigma}_z, \underline{\sigma}_z) + (\sin \alpha) \text{diag}(\underline{\sigma}_y, \underline{\sigma}_y^*) \quad (4)$$

with ϕ being the angle between the barrier magnetic moment and the bulk magnetization (z -axis) as indicated in Fig. 1. Above, $\underline{\sigma}_j$ denotes the j 'th Pauli matrix in spin space. We have defined $\underline{\gamma}_T^{l,r} = R_B^{l,r}/R_F$ and $\underline{\gamma}_s^{l,r} = 1/(R_N G_s^{l,r})$, where R_N is the normal-state resistance of the N region, $R_B^{l,r}$ is the barrier resistance at the left/right interface, while $G_s^{l,r}$ accounts for the spin-dependent interfacial phase-shifts at the left/right interface. In the S region, we make use of the bulk solution for the Green's function

$$\hat{g}^{l,r} = \begin{pmatrix} c & 0 & 0 & se^{\pm i\chi/2} \\ 0 & c & -se^{\pm i\chi/2} & 0 \\ 0 & se^{\mp i\chi/2} & -c & 0 \\ -se^{\mp i\chi/2} & 0 & 0 & -c \end{pmatrix}, \quad (5)$$

where $c = \cosh \theta$, $s = \sinh \theta$, $\theta = \text{atanh}(|\Delta_0|/\varepsilon)$, and the superconducting phase difference is χ . This approximation is valid for low transparency interfaces in which case the proximity effect is weak. The above equations constitute a closed set which may be solved numerically, and we add a small imaginary part to the quasiparticle energy for improved numerical stability, i.e. $\varepsilon \rightarrow \varepsilon + i\delta$ with $\delta/\Delta_0 = 0.01$. To model the experimental situation in Ref.¹², we consider the weak proximity effect regime with a low-barrier transparency and an exchange field h . Specifically, we choose $\underline{\gamma}_T^{l,r} = 40$ and $h/\Delta_0 = 80$ which is within the regime of validity for quasiclassical theory when assuming $\Delta_0 \simeq 1$ meV. Also, in this regime one may safely neglect magnetoresistance terms $\underline{\gamma}_{MR}$ in the boundary conditions¹⁶. We have chosen a numerical approach here to avoid overburdening the paper with cumbersome analytical expressions.

It was proposed by Sprungmann *et al.*¹² that the microscopic mechanism generating the triplet supercurrent was the specific magnetization profile in the Cu_2MnAl layer, featuring a canted magnetization texture near the interface regions. An important observation in Ref.¹² was that the triplet supercurrent was only observed in a limited thickness range, and died off rapidly above a critical thickness L_c thus leaving behind only the conventional short-ranged Josephson current. This indicates that the misalignment angle of the interface magnetization compared to the bulk depends on the thickness L of the layer. Such a conjecture agrees with the fact that the Heusler layers gradually make a transition near the interfaces from pure spin-glass to coexisting spin-glass order with a ferromagnetic moment of increasing magnitude as the thickness increases. To phenomenologically model such behavior, we write the misalignment angles shown in Fig. 1 as

$$\alpha = \alpha_0/[1 + e^{\zeta(L-L_c)}], \quad (6)$$

where α_0 is the misalignment angle at the onset of ferromagnetic order and $\zeta \ll 1$ accounts for the slope with which the canted moments relax into the same orientation as the bulk magnetization.

Let us further qualify¹⁷ the model employed here for the canted interface magnetization texture. A thin film Heusler alloy features a spin glass structure if the film is sputtered at room temperature. Annealing will induce a transposition of nearest-neighbour atoms and tries to drive the compound into a ferromagnetically coupled structure. The maximum ordering effect is achieved within the core of the layer, whereas at the interfaces this ordering process is disturbed due to *e.g.* interdiffusion. Here, an antiferromagnetic Mn-Mn-coupling will persist locally and competes with the ferromagnetic ordering. This causes the mentioned canting of the magnetization axis defined by the one of the core. The issue of what the magnetization profile looks like at the interfaces of thin Heusler layers was investigated experimentally in Ref.¹⁸. We here also briefly mention a theoretical work on the influence of disorder in Co-based Heusler alloys by Picozzi *et al.*¹⁹, although the comparison should be considered carefully since in Co-based Heuslers the Co contributes effectively to ferromagnetism whereas Cu does not carry any magnetic moment in the relevant structure.

We are now in a position to calculate the normalized critical current density of the junction, which in the weak-proximity effect regime is obtained via

$$j_c/j_0 = \max_{\chi} \left| \int_0^\infty d\varepsilon \tanh \frac{\beta\varepsilon}{2} \sum_j \text{Re}\{\mathcal{M}_j\} \right|, \quad j = \{\pm, \sigma = \uparrow, \downarrow\}, \quad (7)$$

where we have defined

$$\begin{aligned} \Delta_0 M_{\pm}/\xi &= [f_{\pm}(-\varepsilon)]^* \partial_x f_{\mp}(\varepsilon) - f_{\pm}(\varepsilon) \partial_x [f_{\mp}(-\varepsilon)]^*, \\ \Delta_0 M_{\sigma}/\xi &= [f_{\sigma}(-\varepsilon)]^* \partial_x f_{\sigma}(\varepsilon) - f_{\sigma}(\varepsilon) \partial_x [f_{\sigma}(-\varepsilon)]^*. \end{aligned} \quad (8)$$

Here, $\{f_t, f_s, f_{\uparrow}, f_{\downarrow}\}$ denote the $S_z = 0$ triplet, singlet, and equal spin-pairing anomalous Green's function induced in the F region, and we have defined $f_{\pm} = f_t \pm f_s$. To make direct

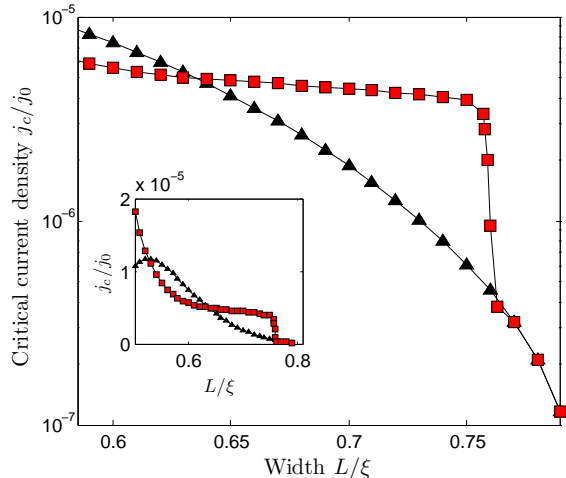


FIG. 2: (Color online) Plot of the critical current density vs. the junction width L . Triangles (black) represent results for the case $\alpha = 0$, i.e. no canted interface moments. Squares (red) represent results for misalignment angle α given by Eq. 6. We have set $\alpha_L = \alpha_R$ with $\alpha_0 = \pi/4$ and $\gamma_\phi^{j,r} = 15$. Assuming a superconducting coherence length of $\xi \simeq 14$ nm in dirty Nb¹³, we use $L_c/\xi = 0.76$ to obtain the sharp drop-off near $L = 10.5$ nm as in Ref.¹². *Inset*: Zoom-out version of the current density.

contact with the experiment of Ref.¹², we contrast a situation with $\alpha = 0$, i.e. no canted interface moments, against a situation where the misalignment angle α evolves with the thickness L according to Eq. (6). The result is shown in Fig. 2. The result is seen to be qualitatively in very good agreement with the finding of Ref.¹²: the supercurrent shows little decay upon increasing the thickness L in the regime where the spin-active zones generate a misalignment angle, and then collapses onto the conventional singlet result above a certain thickness L_c . This suggests that the spin-dependent interface properties may play a pivotal role in the generation of the triplet supercurrent. In our picture, the abrupt change in the spin-triplet Josephson current is due to an abrupt change in the angle α in Eq. 6

Another interesting finding in Ref.¹² is the non-monotonic temperature dependence of the critical current observed in the region of widths L where the long-range current is dominant. With $T_c \simeq 8$ K being the critical temperature¹⁷, we plot the current vs. temperature in Fig. 3 for three choices of the width: (i) right below the region of a dominant triplet current ($L = 6.1$ nm), (ii) in the middle of the region of a dominant triplet current ($L = 8.1$ nm and 8.6 nm), and (iii) right after the vanishing long-range current ($L = 10.7$ nm). We again obtain a good match to the results of Ref.¹². It should be mentioned that we do find signs of $0-\pi$ oscillations for some particular choices of intermediate widths L , but the non-monotonic behavior in the regime of a dominant long-range current is nevertheless confirmed. Close examination of the current vs. temperature curves in Ref.¹² reveals a hint of small-scale oscillation superimposed on the overall non-monotonic behavior for some particular widths L . We were not able to reproduce

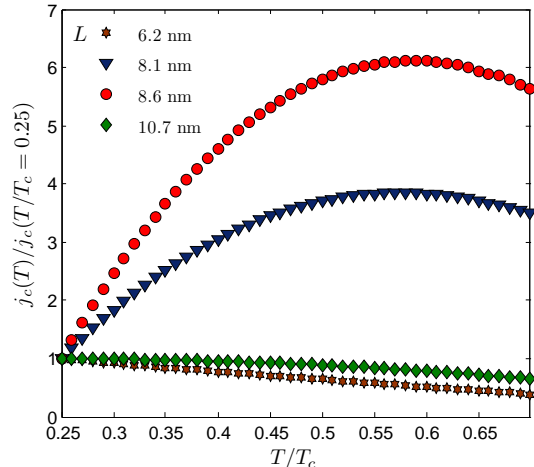


FIG. 3: (Color online) Plot of the critical current density vs. temperature. To make contact with the experiment in Ref.¹² where $T_c \simeq 8$ K, we normalize the current to its value at $T/T_c = 0.25$. The rest of the parameters are as in Fig. 2.

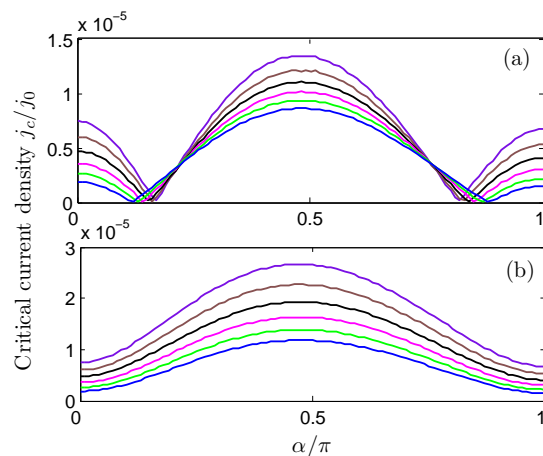


FIG. 4: (Color online) Plot of the critical current density vs. the misalignment angle α in the spin-active zones. In (a), we set $\alpha_L = \alpha_R$ while in (b) $\alpha_L = -\alpha_R$. From top to bottom at $\alpha = \pi/2$, the curves correspond to thicknesses $d_F/\xi = \{0.60, 0.62, 0.64, 0.66, 0.68, 0.70\}$.

these fine-scale oscillations within our model, and speculate that these might pertain to a more complicated magnetization profile in the bulk of the Cu₂MnAl layer since similar behavior has been predicted²⁰ in the conical ferromagnet Ho. We intend to address this issue in a forthcoming work. It should be noted that the spin-dependent phase-shifts occurring at the interfaces can in general influence the $0-\pi$ transition pattern both as a function of the width and temperature of magnetic as well as non-magnetic (normal interlayer) Josephson junctions.

To further highlight the influence on the current density by the presence of a canted magnetization texture near the inter-

faces, we plot in Fig. 4 the current density vs. the misalignment angle in the case of an (a) parallel coupling $\alpha_L = \alpha_R$ between the spin-active zones and an (b) antiparallel coupling $\alpha_L = -\alpha_R$. The main difference between these two cases is that the total supercurrent may actually *vanish* at some misalignment angles when the coupling is parallel. In this scenario, the contribution from the long-range triplet current effectively cancels out the singlet supercurrent. Common for both scenarios is that the maximally attainable critical current occurs near $\alpha = \pi/2$. However, it should be noted that the maximum does not occur exactly at $\alpha = \pi/2$, but rather at a slight off-set $\alpha_c < \pi/2$. When we reverse the bulk magnetization direction, i.e. $h \rightarrow (-h)$, we note that the maximum of the critical current occurs at an angle $\alpha_c > \pi/2$ which is equidistant from $\pi/2$ compared to the former case. This behavior can be understood from a symmetry perspective. Namely, the system is not invariant under a spatial inversion whenever $h \neq 0$ due to the definite direction of the magnetization. Therefore, the angle α_c providing the maximum critical current will either be smaller or larger than $\pi/2$, depending on whether h points along \hat{z} or $-\hat{z}$.

So far, we have constructed a theoretical model for the spin-active zones in the Heusler layer which is able to account well for the experimental finding in Ref.¹². There are nevertheless extensions of this model which could be appropriate to pursue in order to further clarify the underlying physics, and which we comment on. In our treatment, we have included the spin-active zones as effective canted magnetization textures near the interface and included the resulting conductance-terms in the quasiclassical boundary conditions. This is certainly only an effective model for the interplay between spin-glass and ferromagnetic order in the Heusler layers in the interface re-

gion. In a more microscopic lattice-model treatment of the system, one could address how the specific details of such an interplay would influence the critical current behavior. Another issue of interest, is the precise role of the spatially dependent magnetization texture in the ferromagnetic layer. Recent theoretical works²¹ have highlighted the necessary requirements of the magnetization profile which renders possible a long-range triplet current. It would thus be interesting to experimentally extract this profile and its dependence on both spatial coordinate and its evolution in terms of magnetization direction, so that one could construct a more accurate model for this system. Qualitatively, we expect that our model captures the essential features which could account for the generation of a long-range triplet supercurrent in the experimental system of Ref.¹².

In summary, we have constructed a theoretical model to account for recent experimental findings in Ref.¹² which presented evidence for triplet superconductivity in a ferromagnetic Josephson junction with a Cu_2MnAl -Heusler barrier. The crucial ingredients in our model which generate the triplet supercurrent are *spin-active zones* near the interfaces due to a coupling between ferromagnetic and spin glass order, resulting in an effective canted magnetization texture near the interfaces. Using a numerical solution of the quasiclassical equations of superconductivity with spin-active boundary conditions, we find qualitatively very good agreement with the experimentally observed supercurrent. Further experimental implications of the spin-active zones have also been discussed.

Acknowledgments. The authors acknowledge support by the Norwegian Research Council, Grant No. 167498/V30 (STORFORSK), and thank D. Sprungmann for a very useful exchange.

-
- ¹ A. A. Abrikosov and L. P. Gor'kov, Zh. Eksp. Teori. Fiz **39**, 1781 (1960); A. M. Clogston, Phys. Rev. Lett. **9**, 266 (1962); B. S. Chandrasekhar, Appl. Phys. Lett. **1**, 7 (1962).
² F. S. Bergeret *et al.*, Rev. Mod. Phys. **77**, 132 (2005).
³ A. I. Buzdin, Rev. Mod. Phys. **77**, 935 (2005).
⁴ See *e.g.* V. V. Ryazanov *et al.*, Phys. Rev. Lett. **86**, 427 (2001); T. Kontos *et al.*, Phys. Rev. Lett. **86**, 304 (2001).
⁵ See *e.g.* S. S. Saxena *et al.*, Nature **406**, 587 (2000); D. Aoki *et al.*, Nature **4130**, 613 (2001).
⁶ R. S. Keizer *et al.*, Nature **439**, 825 (2006).
⁷ M. Eschrig and T. Löfwander, Nature Phys. **4**, 138 (2008).
⁸ T. S. Khaire *et al.*, Phys. Rev. Lett. **104**, 137002 (2010).
⁹ V. L. Berezinskii, JETP Lett. **20**, 287 (1974).
¹⁰ A. F. Volkov *et al.*, Phys. Rev. Lett. **90**, 117006 (2003).
¹¹ M. Eschrig *et al.*, J. Low. Temp. Phys. **147**, 457 (2007); K. Halterman *et al.*, Phys. Rev. Lett. **99**, 127002 (2007); Y. Tanaka and A. A. Golubov, Phys. Rev. Lett. **98**, 037003 (2007); J. Linder *et al.*, Phys. Rev. Lett. **102**, 107008 (2009).
¹² D. Sprungmann *et al.*, arXiv:1003.2082.
¹³ P. SanGiorgio *et al.*, Phys. Rev. Lett. **100**, 237002 (2008).
¹⁴ N. Schopohl and K. Maki, Phys. Rev. B **52**, 490 (1995).
¹⁵ K. Usadel, Phys. Rev. Lett. **25**, 507 (1970).
¹⁶ D. Huertas-Hernando *et al.*, Phys. Rev. Lett. **88**, 047003 (2002); A. Cottet and W. Belzig, Phys. Rev. B **72**, 180503 (2005).
¹⁷ We thank D. Sprungmann for very helpful communications on this point.
¹⁸ A. Bergmann *et al.*, Phys. Rev. B **72**, 214403 (2005).
¹⁹ S. Picozzi *et al.*, Phys. Rev. B **69**, 094423 (2004).
²⁰ Gabor B. Halasz *et al.*, Phys. Rev. B **79**, 224505 (2009); M. Alidoust *et al.*, Phys. Rev. B **81**, 014512 (2010).
²¹ Ya. V. Fominov *et al.*, Phys. Rev. B **75**, 104509 (2007); M. Houzet and A. Buzdin, Phys. Rev. B **76**, 060504 (2007); I. B. Sperstad *et al.*, Phys. Rev. B **78**, 104509 (2008); A. F. Volkov and K. B. Efetov, Phys. Rev. B **81**, 144522 (2010).